Surface abundance change in vacuum ultraviolet photodissociation of CO_2 and H_2O mixture ices

Takashi Kinugawa,[a] Akihiro Yabushita,[a] Masahiro Kawasaki,*[a] Tetsuya Hama[b] and Naoki Watanabe[b]

[a] *Department of Molecular Engineering, Kyoto University, Kyoto 615-8510, Japan*

[b] *Institute of Low Temperature Science, Hokkaido University, Sapporo 060-0819, Japan*

Photodissociation of amorphous ice films of carbon dioxide and water co-adsorbed at 90 K was carried out at 157 nm using oxygen-16 and -18 isotopomers with a time-of-flight photofragment mass spectrometer. O(^3P_J) atom, OH(v=0) radical, and CO(v=0,1) molecules were detected as photofragments. CO is produced directly from the photodissociation of CO_2. Two different adsorption states of CO_2, *i.e.*, physisorbed CO_2 on the surface of amorphous solid water and trapped CO_2 in the pores of the film, are clearly distinguished by the translational and internal energy distributions of the CO molecules. The O atom and OH radical are produced from the photodissociation of H_2O. Since the absorption cross section of CO_2 is smaller than that of H_2O at 157 nm, the CO_2 surface abundance is relatively increased after prolonged photoirradiation of mixed ice film, resulting in the formation of a heterogenously layered structure in the mixed ice at low temperatures. Astrophysical implications are discussed.

To whom correspondence should be addressed.

Kawasaki@moleng.kyoto-u.ac.jp Phone +81-707-2460 Fax +81-707-2513

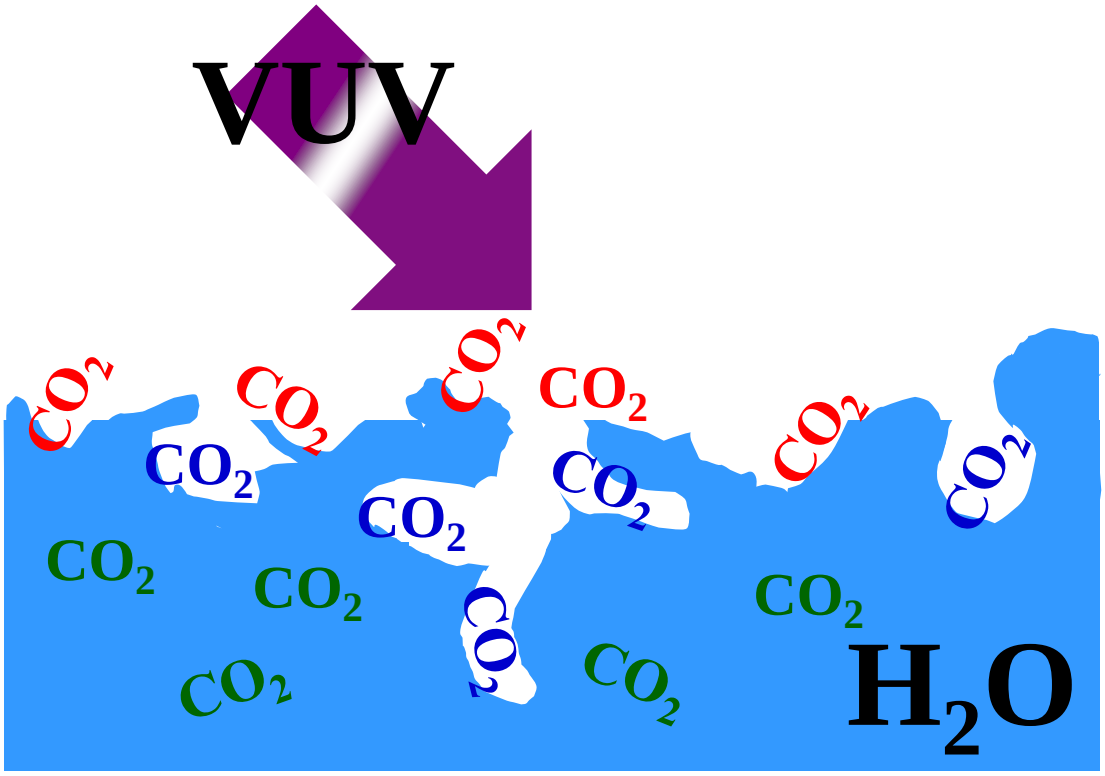

Surface abundance of CO_2 on the surface of CO_2/H_2O mixture ice increases during vacuum ultraviolet photoirradiation at 90 K.

GRAPHICAL CONTENTS ENTRY

1. Introduction

Interactions of gas-phase species with water ice have been of importance in the fields of atmospheric and interstellar chemistry. Following the collision of gaseous species with the surface of water ice, physicochemical processes on the surface proceed, *e.g.*, adsorption on the surface, thermal desorption into the gas phase, diffusion from the surface into the bulk ice, and reaction with other species. Interactions of CO_2 with water ice at low temperature have been studied extensively due to the facts that 1) CO_2 is present in relatively large amounts at low temperatures in a variety of places: the terrestrial mesosphere, the poles of Mars, interstellar clouds and small solar system bodies such as comets or Triton;[1] and 2) CO_2 can be used as a tracer for investigating ice morphology and for studying the trapping and releasing of volatile molecules by water ice. For instance, temperature programmed desorption (TPD) studies showed that two different adsorption states of CO_2 exist in amorphous solid water (ASW). One consists of CO_2 adsorbing atop ASW to make a CO_2 adlayer similar to pure CO_2 ice.[2] The other consists of CO_2 trapped in the cavities of ASW.[3] The latter state has a larger activation energy for desorption than the former state.

The importance of energetic processes caused by vacuum ultraviolet (VUV) photoirradiation is known in the above-mentioned cosmic regions, which can directly induce chemical reactions of the ice mantles. According to Mason et al.,[4] solid CO_2 has smaller absorption cross sections in the VUV region compared with those of solid H_2O. At Lyman-α photons (λ=121.6 nm), for example, cross sections of ~4.0×10^{-18} cm^2 and ~7.0×10^{-19} cm^2 were reported for solid H_2O and CO_2 respectively. This implies that H_2O is efficiently photodissociated compared with CO_2 following VUV photoirradiation of H_2O/CO_2 mixed ice. If such preferential H_2O photodissociation proceeds, and the surface abundance of CO_2 in the mixed ice becomes higher, a layered structure of CO_2 on H_2O may be formed after prolonged irradiation. Photoirradiation on pure or mixed ices triggers desorption of atoms, radicals, or molecules; and the desorption dynamics of photofragments are known to be sensitive to the adsorption states of the photoirradiated molecules. For example, when H_2O molecules are dissociated at λ=157 and 193 nm, the translational energy distributions of the photodesorbed H atoms strongly depend on the morphologies of the ice films as well as the secondary surface reactions.[5,6] Therefore, how the surface composition changes after VUV photoirradiation needs to be known in order to develop detailed modeling of gas-ice interactions including the reactivity of surface reactions.

In the present work, we have measured time-of-flight (TOF) spectra and rotationally resolved resonance-enhanced multiphoton ionization (REMPI) spectra of photodesorbed CO species from 157 nm photoirradiation of mixed CO_2/H_2O ice films at 90 K. Photodesorption processes of OH and O(^3P_J) were also investigated and are further discussed. Two different deposition gas mixtures were used for the mixed ice preparation to investigate the correlation between the CO_2 adsorption structures in the mixed CO_2/H_2O and the photodesorption dynamics.

2. Experimental

2.1. Apparatus and preparation of ice

Our experimental setup consisted of an ultrahigh vacuum chamber, two pulsed molecular flow sources, an excimer laser, and a dye laser. The experiment is concisely described here, but a more detailed explanation of the

experimental apparatus is described elsewhere.[7] The vacuum chamber was evacuated to a base pressure of 10^{-8} Torr by turbo molecular pumps in tandem (Shimadzu, 800 and 50 L s^{-1}). An optically flat sapphire disk substrate (12 mm dia., 2 mm thick), sputter coated with a thin polycrystalline film of Au(111), was supported in the center of the chamber by a liquid-nitrogen-cooled manipulator.

Two types of ASW mixture samples were prepared at 90 K: $C^{16}O_2/H_2{}^{16}O$ and $C^{18}O_2/H_2{}^{16}O$. Co-adsorbed mixture ices were prepared by backfilling deposition of H_2O vapor and CO_2 gas onto the substrate at 90 K by two pulse valves (General Valve). Pulsed molecular flows were introduced simultaneously into the chamber at the rate of 10 Hz. In order to spread vapors all over the chamber, a flat plate was attached in front of each pulse valve. The exposure was typically 900 L (1 L = 1×10^{-6} Torr s) and the mixing ratios of H_2O and $C^{16}O_2$ or $C^{18}O_2$ ranged from 1:4 to 4:1 (typical ratio). Hereafter unless otherwise stated, O atom stands for ^{16}O atom.

In our experimental conditions, CO_2 can exist in two different forms on surface: 1) CO_2 adlayer adsorbed atop the mixture ice film[2,3] and 2) CO_2 trapped in the porous sites.[8,9] To investigate the photodynamics of the CO_2 adlayer on the surface, a prepared CO_2/H_2O mixture ice film was continually exposed to CO_2 gas during pulsed photoirradiation. In these intermittent sequential deposition experiments, the pulse valve for CO_2 was opened after each laser shot so as to deposit fresh CO_2 layers on the CO_2/H_2O mixture ice film. Hereafter, experiments using thus prepared ice samples are called "CO_2 adlayer" experiments. The term adlayer refers to the layers of CO_2 atop the ASW surface. For investigation of the photodynamics of CO_2 trapped in the CO_2/H_2O mixture ice film, fresh layers of the CO_2/H_2O mixture ice film were adsorbed by intermittent refreshment with the CO_2 and H_2O gases. In the present experiment, the two pulse valves for CO_2 and H_2O gases were opened after each laser shot to prepare a fresh layer of the CO_2/H_2O mixture ice. Hereafter, experiments using thus prepared ice samples are called "fresh CO_2/H_2O" experiments. The intermittent refreshments of the ice films exclude a potential influence of photoproducts such as H_2CO_3 accumulated on the mixed ice surface by 157 nm photoirradiation on the energy distributions of measured photoproducts.[10] All of the present experiments were performed at a sample temperature of 90 K, and a typical chamber pressure for intermittent experiments was 5×10^{-7} Torr. The pressure without fresh deposition was 5×10^{-8} Torr.

Unfocused 157 nm laser radiation was incident at an angle of about 80° to the surface normal the ice surface at a fluence < 0.1 mJ cm^{-2} $pulse^{-1}$. CO photoproducts were subsequently ionized at a vertical distance of 3 mm normal to the substrate surface by 2 + 1 REMPI via the $B\ ^1\Sigma^+$ (v' = 0,1) ← $X\ ^1\Sigma^+$ (v'' = 0,1) sequential vibrational transitions at 229.90 - 230.35 nm, and collected with a small mass spectrometer aligned perpendicular to the ice surface.[11,12] OH and O(^3P_J) were detected by 2 + 1 REMPI via the OH($D\ ^2\Sigma^-$ ← $X\ ^2\Pi$) transition at 244.0 - 244.5 nm,[13] and the O($3p\ ^3P_J$ - $2p\ ^3P_J$) transition at 225.6 - 226.4 nm.[14] PGOPHER, a program for simulating rotational structure, was used to estimate the rotational temperatures of the photoproducts.[15] Spectroscopic parameters were taken from Greenslade et al.[16] and Huber and Herzberg for OH,[17] and Huber and Herzberg,[17] Morton et al.,[18] and Chen and Yeung for CO.[19]

2.2. Simulation of time-of-flight spectra of CO photoproducts

The TOF spectra of photoproducts were taken as a function of delay time between the photolysis and REMPI laser

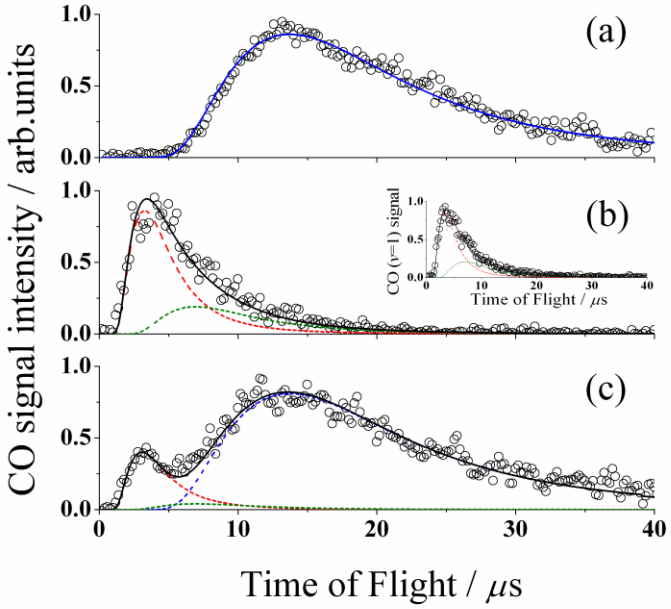

Fig. 1 TOF spectra of CO [$B\ ^1\Sigma^+(v' = 0) \leftarrow X\ ^1\Sigma^+\ (v'' = 0)$] following 157 nm photoirradiation of (a) fresh CO_2/H_2O mixture ice at 90 K for which CO_2 and H_2O are co-adsorbed with keeping the surface fresh. (b) CO_2 adlayer for which CO_2 are sequentially adsorbed on the surface of the CO_2/H_2O mixture ice, the inset shows the TOF spectrum of CO(v=1). (c) CO_2/H_2O mixture after 1 hr photoirradiation. The solid curves are fits to the data derived with T_{trans} = 1600 (red), 350 (green), and 90 K (blue). Probe laser wavelengths are 230.101 nm for (a) and 230.092 nm for (b, c).

pulses using a delay generator to investigate the translational energies of desorbing photoproducts. Details regarding the simulation of such TOF spectra have been reported previously.[7] The measured TOF spectra $S(a_i, t, T_{trans})$ of the photoproducts were fit to a sum of one or more flux-weighted Maxwell - Boltzmann (MB) distributions S_{MB}, each defined by a translational temperature T_{trans}. The coefficients, a_i, are used for the relative population of each MB distribution,

$$S(a_i, t, T_{trans}) = \Sigma a_i S_{MB}(t, T_{trans}), \quad (1)$$

$$S_{MB}(t, T_{trans}) = r^3 t^{-4} \exp[- mr^2/2k_B T_{trans} t^2], \quad (2)$$

$$P_{MB}(E_{trans}) = (k_B T_{trans})^{-2} E_{trans} \exp[-E_{trans}/k_B T_{trans}], \quad (3)$$

where r is a flight length of photoproducts. The MB distribution $P_{MB}(E_{trans})$ as a function of translational energy E_{trans} is characterized by the averaged translational energy $<E_{trans}>=2k_B T_{trans}$, where k_B is the Boltzmann constant. The Jacobian given by Zimmerman and Ho was used to obtain the translational energy distribution from the TOF distribution.[20] A small contribution of very slow TOF component (T_{trans}=20±5 K) appeared after t=20 μs. This component is considered to be an artifact caused by the CO photofragments that were scattered once and bounced back to the REMPI detection region. This slowest component was subtracted from the TOF spectrum simulating MB distributions.

Table 1 Translational and rotational temperatures of CO(v=0) photofragments.

	Temperatures / K	
	Translation	Rotation
fresh CO_2/H_2O	90 ±10 (100%)	150 ±50 [b]
CO_2 adlayer	1600 ±400 (70%) 350 ±50 (30%)	800 ±200 [a] —
CO_2/H_2O after photoirradiation	1600 ±400 (11%) 350 ±50 (2%) 90 ±10 (87%)	800 ±200 [a] — 150 ±50 [b]

Numbers in parentheses are contributions of each temperature component in TOF spectra.

—: not measured

[a] TOF=3.0 μs.

[b] TOF=12.0 μs.

3. Results

3.1. CO photoproducts

Figure 1 shows typical TOF spectra of CO(v=0) following 157 nm irradiation on (a) fresh CO_2/H_2O mixture, (b) CO_2 adlayer and (c) CO_2/H_2O mixture after 1 hour 157 nm photoirradiation without refreshment, which were measured at a REMPI wavelength of the Q-head. The spectrum (a) is well reproduced by a single MB distribution with T_{trans}=90±10 K. The spectrum (b) is reproduced with T_{trans}=1600±400 K (70%) and 350±50 K (30%), while the T_{trans}=90 K component is not observed. The spectrum (c) consists of three MB distributions with T_{trans}=1600±400 (11%), 350±50 (2%) and 90±10 K (87%). Table 1 summarizes the results.

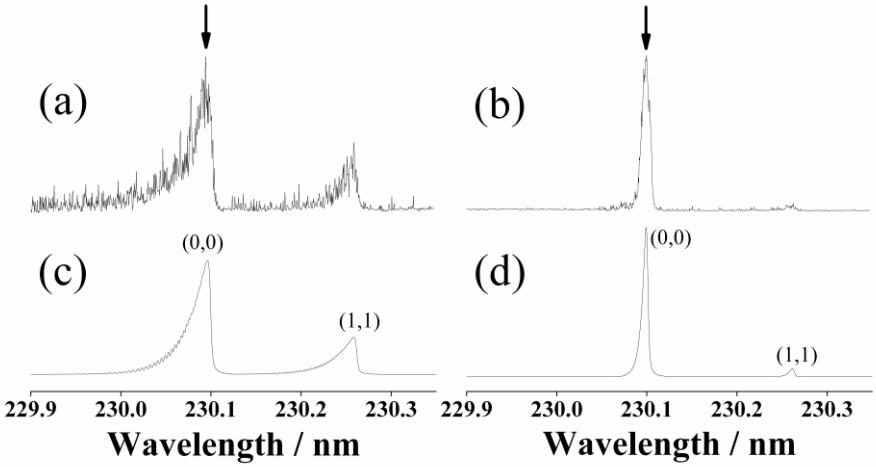

Fig. 2 REMPI excitation spectra of the CO $B\ ^1\Sigma^+ \leftarrow X\ ^1\Sigma^+$ transition from CO_2/H_2O mixture ice at 90 K, (a) at time-of-flight t=3.0 μs and (b) t=12.0 μs. The arrows indicate the Q-heads used for time-of-flight measurements in Fig. 1(c) and (d): Spectral simulation assuming Boltzmann rotational state population distributions with (c) T_{rot}=800 K and (d) 150 K.

Figures 2(a) and (b) show REMPI excitation spectra of CO from CO_2/H_2O mixture after 1 hr irradiation at 157 nm at (a) t=3.0 μs and (b) 12.0 μs, respectively. The rotational temperatures T_{rot} of CO(v=0) are estimated to be 800±200 and 150±50 K for t=3.0 and 12.0 μs, respectively, by spectral simulations as shown in Figs. 2(c) and (d). Figures 3(a) and (b) show time evolutions of CO(v=0) from a CO_2/H_2O mixture left under vacuum at 90 K for 1 minute after preparation of the ice at (a) t=3.0 μs for CO(T_{trans}=1600 K) and (b) t=12.0 μs for CO(T_{trans}=90 K) as a function of 157 nm irradiation time. These two signals immediately appeared after 157 nm irradiation. After initial rise of the signals, the CO(T_{trans}=1600 K) intensity increased with 157 nm irradiation time, while the CO(T_{trans}=90 K) intensity stayed constant. Figure 3(c) shows time evolution of CO(v=0) from CO_2/H_2O mixture when the ice sample was left under vacuum without photoirradiation at 90 K for 10 minute after ice preparation. Even for 20 min waiting time, the qualitatively same signal evolution was observed. In contrast to the above mentioned results, both the fast and slow signals do not promptly appear and their intensities increase gradually with irradiation time at 157 nm. CO_2 desorption from pure CO_2 ice at 90 K was studied experimentally and

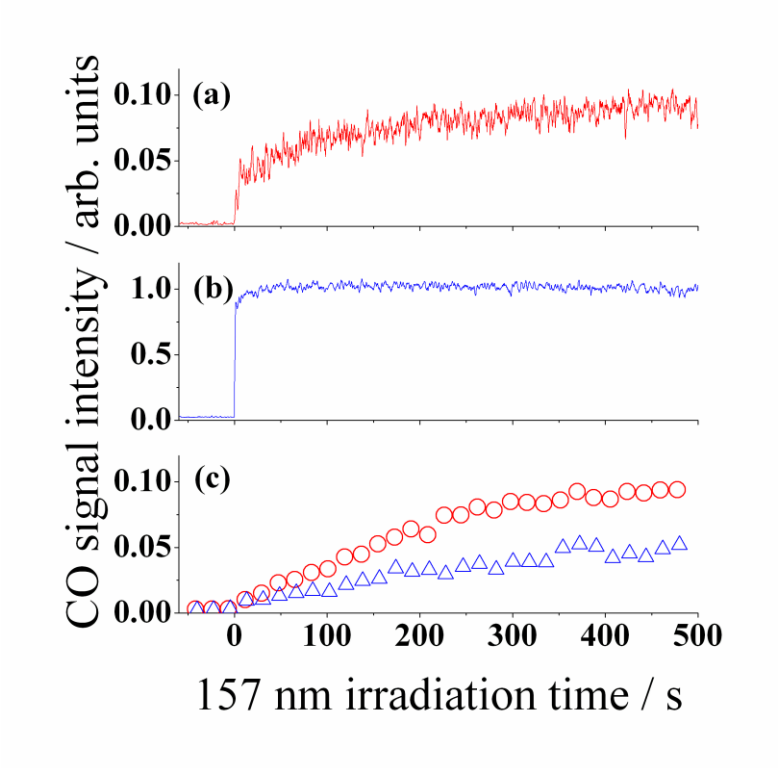

Fig. 3 Time evolutions of CO [$B\ ^1\Sigma^+$ (v'=0) ← $X\ ^1\Sigma^+$ (v''=0)] from CO_2/H_2O mixture ice left under vacuum at 90 K for one-minute after ice preparation as a function of 157 nm irradiation time (a) at t = 3.0 μs at 230.092 nm, (b) at t=12.0 μs at 230.101 nm. (c) the mixture ice sample was left under vacuum without photoirradiation for ten min at 90 K after ice preparation, and it should be noted that relative intensities of the fast and slow components cannot be quantitatively compared to each other.

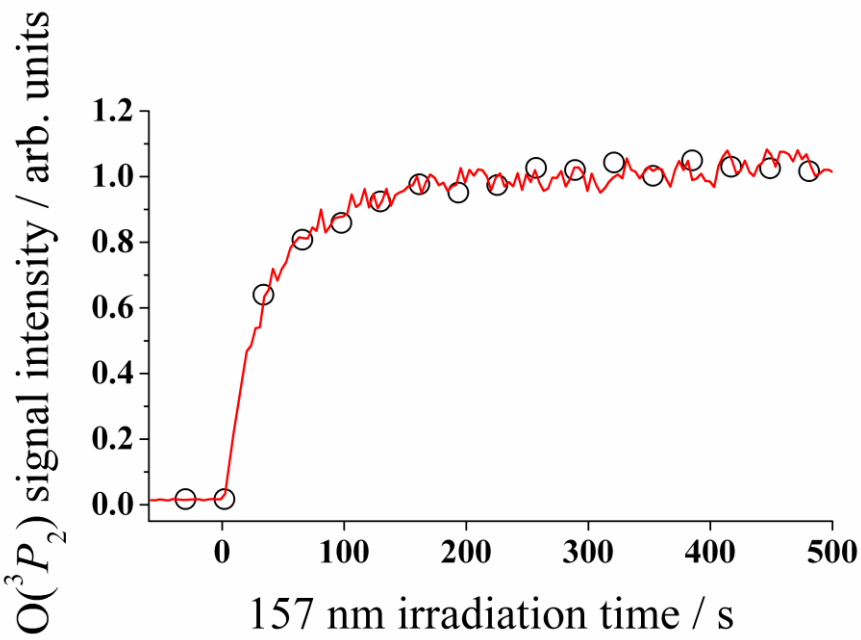

Fig. 4 Time evolutions of O($^3P_2$) from CO_2/H_2O mixture ice (red line) and from neat ASW(H_2O) (open circle) as a function of 157 nm irradiation time at TOF=1.5 μs.

theoretically by Mate et al.[2] A film of pure CO_2 ice of approximately 180 nm was deposited on the Al substrate at 90 K. Once the CO_2 deposition was stopped, CO_2 began to desorb. However, CO_2 still remained on the substrate at least 30 minute after the deposition. Our previous experimental results suggest that the effect of further deposition of H_2O from residual gas to suppress an initial photolysis of CO_2 on the ice surface was negligible.[21]

3.2. O(^3P_J) atom from CO_2/H_2O mixture and CO_2 adlayer

Figure 4 shows the time evolution of O($^3P_2$) from a CO_2/H_2O mixture one-minute after preparation of the ice as a function of 157 nm irradiation time at 225.655 nm at t=1.5 μs corresponding to the maximum in its TOF spectrum. For comparison purpose, Fig. 4 includes the time evolution data of O($^3P_2$) from ASW(H_2O) at t=1.5 μs, which corresponding to the maximum in its TOF spectrum from 157 nm photodissociation of neat ASW(H_2O), from which O(^3P_J) are produced.[22]

The evolution behaviors of O($^3P_2$) from CO_2/H_2O mixture and ASW(H_2O) are in good accordance to each other. The branching ratio of angular momentum states of O(^3P_J) from CO_2/H_2O mixture after 1 hr irradiation at 157 nm was 2.4 : 1.8 : 1 for J=2, 1, 0, which is in accordance with that from ASW(H_2O). To further confirm the O($^3P_2$) source, photoirradiation of the $C^{18}O_2$/$H_2{}^{16}O$ mixture was made, in which detection of ^{18}O(^3P_J) was not successful because strong ^{16}O(^3P_J) signal disturbed weak ^{18}O(^3P_J) signal, while $C^{18}O$ was successfully detected at t=3.0 μs. These results suggest that the main O($^3P_2$) source from the CO_2 doped H_2O ice film is not CO_2 but H_2O. Note that a weak signal of ^{18}O(^3P_J) was successfully detected from neat $C^{18}O_2$ adlayer experiment. This result suggests that CO_2 dissociates mainly to CO + O(^1D) and to only a small extent CO + O(^3P_J). Also that electronic quenching of O(^1D) to O(^3P_J) on the ASW surface plays only a minor role in the present photodesorption study. Zhu and Gordon

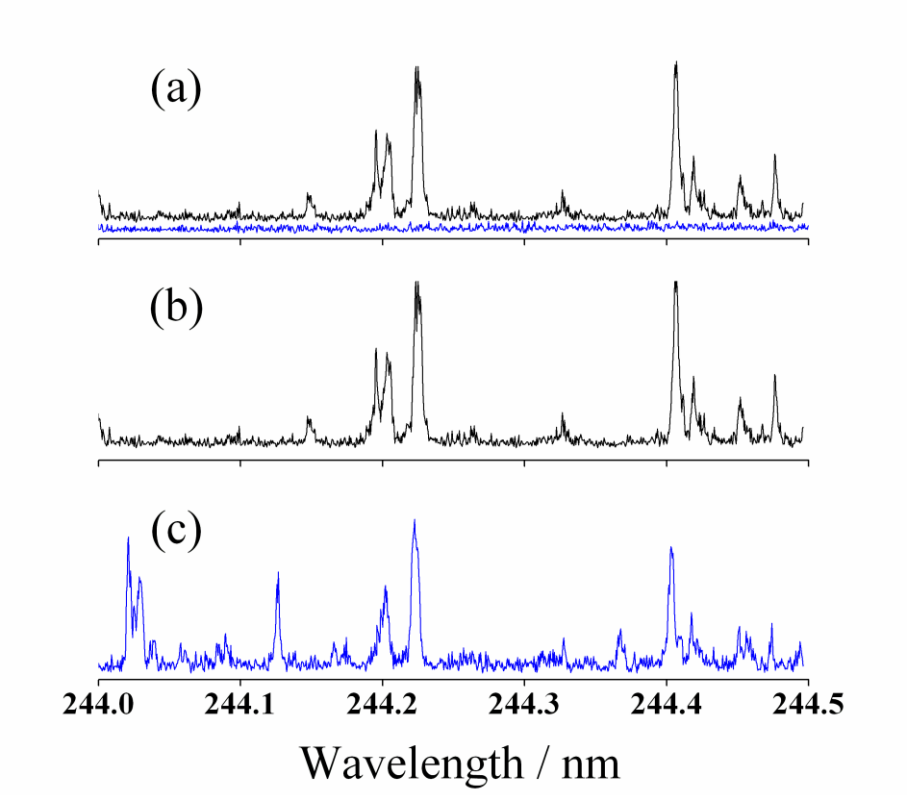

Fig. 5 REMPI excitation ($D\ ^2\Sigma^- \leftarrow X\ ^2\Pi$) spectra of ^{16}OH and ^{18}OH from ice samples after 1 hour 157 nm photoirradiation at t = 1.0 μs. (a) m/z = 17 (black) for ^{16}OH and m/z = 19 (blue) for ^{18}OH from $C^{18}O_2/H_2{}^{16}O$ mixture ice. (b) ^{16}OH and (c) ^{18}OH from $H_2{}^{18}O/H_2{}^{16}O$.

reported that the yield of the O(^3P) production is 0.05 at 157 nm in the gas phase by a chemical scavenging technique,[23] which is confirmed by a molecular beam photofragment spectroscopy study by Stolow and Lee.[24] O(^1D) is known to react easily with parent H_2O molecules by collisions with ASW to produce OH or H_2O_2.[25,26] CO_3 could be transiently formed through reaction of O(^1D) with CO_2, but it is reported to be stable only at lower than 50 K.[27]

Table 2 O($^3P_2$) and OH from amorphous solid water and CO_2/H_2O isotopomer mixture ice

	Photofragments			
	$^{16}O(^3P_2)$ [a]	$^{18}O(^3P_2)$ [a]	^{16}OH [b]	^{18}OH [b]
$C^{16}O_2/H_2{}^{16}O$ after photoirradiation	○	—	○	—
$C^{18}O_2$ adlayer on $C^{18}O_2/H_2{}^{16}O$	○	○	—	—
$C^{18}O_2/H_2{}^{16}O$ after photoirradiation	○	○	○	×
$H_2{}^{18}O/H_2{}^{16}O$ after photoirradiation	○	○	○	○

○ : observed, ×: not observed, —: not measured

[a] TOF=1.5 μs.

[b] TOF=1.0 μs.

3.3. OH desorption from photoirradiation of $C^{18}O_2/H_2{}^{16}O$ mixture, neat ASW($H_2{}^{18}O$) and neat ASW($H_2{}^{16}O$)

Figure 5(a) shows REMPI excitation spectra of ^{16}OH from $C^{18}O_2$/ $H_2{}^{16}O$ mixture after 1 hr 157 nm irradiation without intermittent deposition, while ^{18}OH was not detected. It is well known that H_2O_2 or H_2CO_3 were formed following energetic particle irradiations of pure H_2O and CO_2/H_2O mixed ice, respectively.[10,21,28-30] Recognizing that these photoproducts would accumulate on the ice surface after prolonged irradiation by 157 nm photolysis pulses, we have also confirmed that weak ^{16}OH was also successfully detected from fresh $C^{18}O_2/H_2{}^{16}O$ mixture. These results suggest that $H + C^{18}O_2 \rightarrow {}^{18}OH + CO$ reaction does not occur efficiently. To confirm that our REMPI system could detect OH isotopomers, REMPI excitation spectra of ^{16}OH from ASW($H_2{}^{16}O$) and ^{18}OH from ASW($H_2{}^{18}O$) were measured as shown in Figs. 5(b) and (c). These spectra were taken at t = 1.0 μs corresponding to the TOF maximum of the OH formed via 157 nm irradiation of ASW (H_2O) which both nascent H_2O and photoproduced H_2O_2 contribute to OH photodesorption.[10] Table 2 summarizes the results of the isotope experiments.

4. Discussion

4.1. Adsorption states of CO_2 and relevant photodissociation dynamics

In the present study, CO_2/H_2O mixture ice films were continually refreshed by intermittent exposure to CO_2 gas (CO_2 adlayer experiment) and CO_2/H_2O mixture gas (fresh CO_2/H_2O experiment) during pulsed photoirradiation to investigate CO_2 adsorption structures on ASW and their effects to the CO_2 photodynamics. Our experimental results showed that the translationally and internally hot CO (T_{trans}=1600 K, T_{rot}=800 K) components were observed in the CO_2 adlayer experiment, while cold (T_{trans}=90 K, T_{rot}=150 K) components appeared in the fresh CO_2/H_2O experiment. Adsorption and inclusion states of CO_2 on or in water ice at low temperature have been reported extensively. For crystalline water ice, the Arrhenius activation energy for CO_2 desorption at around 90 K is 0.20 - 0.24 eV with a pre-exponential factor of about 10^{13} s^{-1}, which gives an average residence time = 50 ms at 90 K.[2,31-33] However, the residence time for CO_2 trapped in the pores of ASW was estimated to be on the order of a few minutes, corresponding to a desorption activation energy of about 0.3 eV.[33] Maylk et al. found two different

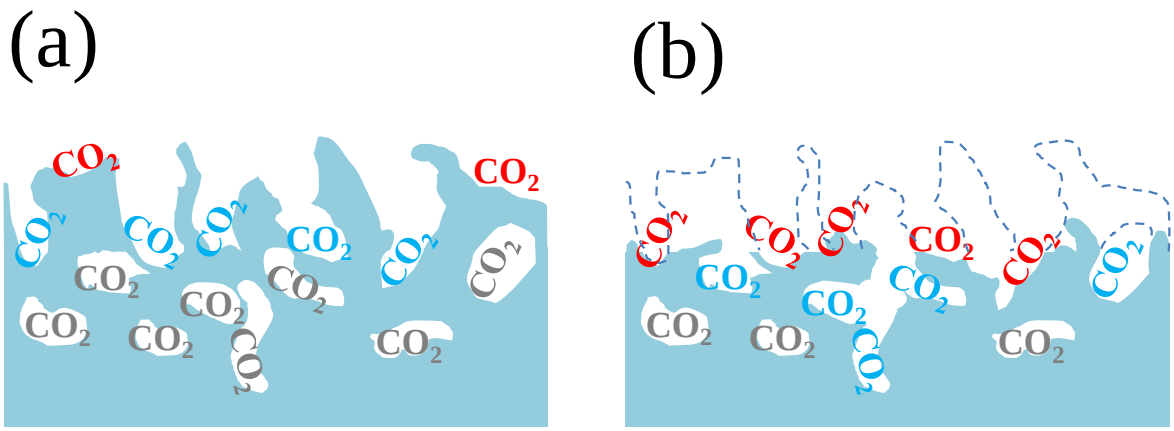

Fig. 6 Schematic illustration of the distribution of CO_2 in CO_2/H_2O mixture ice, (a) as deposited before irradiation and (b) after prolonged 157 nm irradiation. CO_2 (red) stand for physisorbed CO_2 on surface, CO_2 (blue) are trapped in the pore and CO_2 (gray) are buried in the bulk phase. Due to the smaller absorption cross section of CO_2 than that of H_2O, the surface abundance of CO_2 increases after prolonged 157 nm photoirradiation. The fast time-of-flight component comes from CO_2 (red), while the slow one from CO_2 (blue).

CO_2 structures on the surface of the mixture ice in their TPD experiments: 1) adsorbed atop water ice surface, which evaporates at sublimation temperature of pure CO_2, and 2) trapped in the cavities desorbing during the amorphous-to-cubic ice phase transition.[3] Figure 6(a) schematically shows these two different structures. Sandford and Allamandola investigated the condensation and vaporization properties of CO_2 in H_2O/CO_2 mixed ice for various mixing ratios using infrared spectroscopic technique.[32] For ices with $H_2O/CO_2 > 20$, the CO_2 is trapped in the strong hydrogen-bonded amorphous H_2O lattice with interconnecting molecular pores. Little CO_2 is lost until the sublimation temperature of the H_2O matrix is reached. In contrast, in ice having $H_2O/CO_2 < 5$, the CO_2 remains only to the temperature of about 90 K.[32] These reported results indicate that 1) in the present CO_2 adlayer experiments, the ice surface is covered with a mono- or multilayered CO_2 during the intermittent injection of neat CO_2 gas into the vacuum chamber, which has a short residence time, and 2) for the fresh CO_2/H_2O mixture experiment, on the contrary, CO_2 is physically trapped in the strong hydrogen-bonded amorphous H_2O lattice with interconnecting molecular pores, which has a long residence time. We propose that the translationally fast (T_{trans}=1600 K) and internally hot (T_{rot}=800 K) CO component observed in the CO_2 adlayer experiments comes from CO_2 adsorbed atop water ice surface. The translationally slow (T_{trans}=90 K) and internally cold (T_{rot}=150 K) CO component observed in the fresh CO_2/H_2O mixture experiment is due to energy relaxation process by collisions within the inner surface of the mixed ice *en route to* the vacuum, since it is trapped on the porous sites.

Once 157 nm irradiation started, both CO(T_{trans}=1600 and 90 K) components appeared immediately from the CO_2/H_2O mixture film that was left for 1 min after the preparation, as shown in Figs. 3(a) and (b), suggesting that both CO_2 adsorbed atop water ice surface and CO_2 trapped in pores could survive for at least 1 min on the ice surface. Based on the facts that 1) CO(T_{trans}=1600 K) intensity increased with 157 nm irradiation time as shown in Fig. 3(a), and 2) both the fast and slow CO signals do not promptly appear when the CO_2/H_2O mixture was left under vacuum at 90 K for 10 minute before 157 nm photoirradiation, we infer that a) the effective residence time of

CO_2 adsorbed on the top surface, which generates CO(T_{trans}=1600 K), is > 0.1 s (corresponding to a 157 nm laser pulse rate of 10 Hz) at 90 K, and b) CO_2 on the ice surface were desorbed into vacuum during 10 minute. These numbers are in fair agreement with the reported residence times, ~50 ms for CO_2 on crystalline ice surface and a few min for CO_2 in the pores at 90 K.[33] Possibility of thermal segregation of CO_2 molecules during waiting time will be discussed below.

4.2. Formation of inhomogeneous layer structures by photoabsorption at 157 nm

An UV absorption cross section of ASW is ~5×10^{-19} cm^2 at 157 nm.[4] Mason et al. also reported the absorption cross section of solid CO_2, ~5×10^{-20} cm^2 at 157 nm, which is about one order of magnitude smaller than that of ASW.[4] Since CO_2 has the smaller absorption cross section than H_2O, the surface abundance of CO_2 in the mixed ice film is expected to become higher after prolonged 157 nm photoirradiation. This induces surface state change after photoirradiation. Actually, as shown in Figs. 3(a) and (b), the CO(T_{trans}=1600 K) intensity increased with 157 nm irradiation time, while CO(T_{trans}=90 K) intensity has no appreciable temporal change. These results indicate an increase of the surface abundance of the CO_2 adlayer adsorbed atop the CO_2/H_2O mixture ice at 90 K presumably by the preferential H_2O photodissociation. This surface state change of CO_2 after photoirradiation is schematically illustrated in Fig. 6.

One might consider that CO_2 molecules could be thermally segregated at 90 K from the bulk ice to the surface, which result in increase of the surface abundance of CO_2.[34] However, Fig. 3(c) shows both the fast and slow CO signals do not promptly appear when the CO_2/H_2O mixture was left under vacuum at 90 K for 10 minute before photoirradiation started, and also their intensities increase gradually with 157 nm photoirradiation time. These results indicate desorption of CO_2 into vacuum occurs more efficiently than the thermal surface-segregation during the 10 minute waiting time, and also the 157 nm photoirradiation induced the increase of the surface abundance of the CO_2 on the ice samples. The same results were obtained for 20 min waiting time.

Another possible reason for the increase of CO_2 abundance on the CO_2/H_2O mixture ice surface would be that CO_2 may be transferred from the bulk ice to the top surface by photo-induced local heating by pulsed 157 nm photoirradiation. The thermal consequence of pulsed laser irradiation was discussed by Yardley[35] and Osmundsen et al.[36] The optical depth for a 157 nm photon in an H_2O ice, or the depth to which the UV transmission drops to $1/e$ = 37%, is ~100 nm, and the reflectivity R = 0.06.[37] Assuming a square incident laser pulse with a pulse width of τ (second), then the maximum temperature (K) rise of the surface is

$$\Delta T = 2I\,(1 - R)\,(1 - 1/e)\,(\beta\tau/\pi)^{1/2} / \kappa, \qquad (4)$$

where R is the surface reflectivity at the laser wavelength, and I $(1 - R)$ $(1 - 1/e)$ is the energy absorbed in the optical depth (~100 nm). For the ASW ice, density $\rho = 9.4\times10^{-1}$ g cm^{-3},[38] thermal conductivity $\kappa = 7.2\times10^{-2}$ J s^{-1} cm^{-1} K^{-1},[38] heat capacity $c = 7.9\times10^{-1}$ J g^{-1} K^{-1},[39] and $\beta = \kappa/\rho c = 9.7\times10^{-2}$ s^{-1} cm^2. Assuming 157 nm laser intensity $I = 1 \times 10^4$ J s^{-1} cm^{-2}, and pulse width $\tau = 10^{-8}$ s, then the maximum temperature rise is 2.9 K in 100 nm of ASW layer. This temperature rise would not enhance thermal processes at the surface. In fact, we have previously checked the possible influence of photoirradiation on an ASW surface if the partial annealing or modifications of the ice surface might occur by 157 nm laser irradiation.[21] As a result, the ASW surfaces maintained its distinct surface porosity during the 157 nm irradiation experiments at least for 1 hr. Therefore, the local heating by 157 nm photoirradiation

(and deposition of the photon energy of the photoproducts into the ice sample) play only a minor role in the present study.

4.3. Astrophysical implications

The reactivity of surface reactions is strongly affected by the surface composition. For example, Watanabe et al. studied surface reactions of non-energetic H atoms on solid O_2 or CO to understand the formation of water and organic compounds on interstellar grain surfaces, revealing that reactivity of CO hydrogenation is enhanced on ASW at temperatures above ~15 K when compared to pure solid CO.[4] They also report that the hydrogenation reactions become saturated at some stage although some O_2 or CO still remain unreacted. The hydrogenation reaction dominantly occurs at the surface of the solid O_2 or CO, and the formation of an onion-like layered structure by reaction products suppresses the further reactions because hydrogenation hardly proceeds with O_2 and CO buried by the products like H_2O_2 and H_2CO.[40,41] In the case of O_2 hydrogenation, during the H exposure, the reactions construct the layered structure on the sample solid with H_2O on the top, H_2O_2 in the middle, and O_2 at the bottom. However, in the interstellar environments where deposition rates of incoming atoms and molecules are quite low, the reaction-induced formation of layered structure on ice mantles would be inefficient. Our results indicate that the preferential photodissociation of H_2O also can make the layered structure. Since VUV absorption cross sections of CO_2 are smaller than those of H_2O in the entire wavelength region, CO_2 is less efficiently dissociated than H_2O, and CO_2 may be condensed on the surface below the evaporation temperatures of H_2O. The VUV source in interstellar molecular clouds is cosmic-ray pumped hydrogen, and thus, the dominant photoexcitation wavelengths available are H Lyman-α and photons within the Lyman band of H_2. The predicted VUV flux is 1.4×10^3 cm^{-2} s^{-1}.[42] The estimated photon flux at the edge of the solar system is reported to be 9.6×10^7 cm^{-2} s^{-1}.[43] The 157 nm laser used in the present study delivers a fluence of $< 10^{14}$ cm^{-2} $pulse^{-1}$, which roughly corresponds to those in interstellar molecular clouds and Oort cloud 10^4 years and one month, respectively. Considering the residence times of ices in regions 10^7 years for interstellar ice mantles and 10^9 years for cometary ices in Oort cloud,[43] CO_2 is expected to be relatively concentrated on the top surface of such extraterrestrial ices due to the preferential H_2O photodissociation.

5. Summary

We have measured time-of-flight spectra and rotationally resolved REMPI spectra of photodesorbed CO species following 157 nm photodissociation of mixed CO_2/H_2O (1:4) ice films at 90 K. Two different deposition gas mixtures were used for the mixed ice preparation to investigate CO_2 adsorption structures on H_2O ice. Hot CO (v=0,1,T_{trans}=1600 K and T_{rot}=800 K) and cold CO(v=0,T_{trans}=90 K and T_{rot}=150 K) were observed as photodesrobed products, suggesting that the hot CO comes from CO_2 adsorbed atop water ice surface, while CO_2 trapped on the porous sites produces the cold CO component due to an energy relaxation process by collisions within the mixed ice *en route to* the vacuum. Photodesorption of OH and O(^3P_J) was also observed, which is predominantly produced from the photodissociation of H_2O in the mixture ice. Formation of the heterogeneous structures from mixed ice films should depend on photoabsortion cross sections, ice temperatures and photon flux. Since the VUV absorption cross section of CO_2 is smaller than that of H_2O in the entire VUV wavelength region,

CO_2 is less efficiently dissociated than H_2O. After photoirradiation on the CO_2/H_2O mixture ices, CO_2 are relatively condensed on the ice surface at low temperatures.

Acknowledgement

This work was supported by Grants-in-Aid (20245005 and 23684045) from Japan Society for the Promotion of Science

.

References

[1] M. H. Moore, R. L. Hudson and R. F. Ferrante, *Earth, Moon and Planets*, 2003, **92**, 291.

[2] B. Mate, O. Galvez, B. M. Llorente, M. A. Moreno, V. J. Herrero, R. Escribano and E. Artacho, *J. Phys. Chem. A*, 2008**, 112**, 457.

[3] S. Malyk, G. Kumi, H. Reisler and C. Wittig, *J. Phys. Chem. A*, 2007, **111**, 13365.

[4] N. J. Mason, A. Dawes, P. D. Holtom, R. J. Mukerji, M. P. Davis, B. Sivaraman, R. I. Kaiser, S. V. Hoffmann and D. A. Shaw, *Faraday Discuss*., 2006, **133**, 311.

[5] A. Yabushita, D. Kanda, N. Kawanaka, M. Kawasaki and M. N. R. Ashfold, *J. Chem. Phys.*, 2006, **125**, 133406.

[6] A. Yabushita, T. Hama, D. Iida, N. Kawanaka, M. Kawasaki, N. Watanabe, M. N. R. Ashfold and H. P. Loock, *J. Chem. Phys.*, 2008, **129**, 044501.

[7] A. Yabushita, Y. Inoue, T. Senga, M. Kawasaki and S. Sato, *J. Phys. Chem. B*, 2002, **106**, 3151.

[8] A. Bar-Nun, G. Herman, D. Laufer and M. L. Rappaport, *Icarus*, 1985, **63**, 317.

[9] M. P. Collings, M. A. Anderson, R. Chen, J. W. Dever, S. Viti, D. A. Williams and M. R. S. McCoustra, *Mon. Not. R. Astron. Soc*., 2004, **354**, 1133.

[10] T. Hama, A. Yabushita, M. Yokoyama, M. Kawasaki and S. Andersson, *J. Chem. Phys.*, 2009, **131**, 054508.

[11] P. J. H. Tjossem and K. C. Smyth, *J. Chem. Phys*., 1989, **91**, 2041.

[12] S. Wurm, P. Feulner and D. Menzel, *J. Chem. Phys*., 1996, **105**, 6673.

[13] E. de Beer, M. P. Koopmans, C. A. de Lange, Y. Wang and W. A. Chupka, *J. Chem. Phys*., 1991, **94**, 7634.

[14] J. E. M. Goldsmith, *J. Chem. Phys*., 1983, **78**, 1610.

[15] C. M. Western, PGOPHER, a program for simulating rotational structure, University of Bristol, available at http://pgopher.chm.bris.ac.uk.

[16] M. E. Greenslade, M. I. Lester, D. C. Radenovic, A. J. A. van Roji and D. H. Parker, *J. Chem. Phys.*, 2005, **123**, 074309.

[17] K. P. Huber and G. Herzberg, *Molecular Spectra and Molecular Structure IV. Constants of Diatomic Molecules* (Van Nostrand Reinhold, New York, 1979)

[18] D. C. Morton and L. Noreau, *Astrophys. J. Suppl*., 1994, **95**, 301.

[19] K. M. Chen and E. S. Yeung, *J. Chem. Phys*., 1978, **69**, 43.

[20] F. M. Zimmermann and W. Ho, *Surf. Sci. Rep*., 1995, **22,** 127.

[21] A. Yabushita, T. Hama, D. Iida and M. Kawasaki, *J. Chem. Phys*., 2008, **129**, 014709.

[22] T. Hama, A. Yabushita, M. Yokoyama, M. Kawasaki and N. Watanabe, *J. Chem .Phys*., 2009, **131**, 114511.

[23] Y. F. Zhu and R. J. Gordon, *J. Chem. Phys*., 1990, **92**, 2897.

[24] A. Stolow and Y. T. Lee, *J. Chem. Phys*., 1993, **98**, 2066.

[25] E. J. Dunlea and A. R. Ravishankara, *Phys. Chem. Chem. Phys*., 2004, **6**, 3333.

[26] W. Zheng, D. Jewitt and R. I. Kaiser, *Phys. Chem. Chem. Phys*., 2007, **9**, 2556.

[27] C. J. Bennett, C. S. Jamieson and R. I. Kaiser *Phys. Chem. Chem. Phys*., 2010, **12**, 4032.

[28] Z. Peeters, R.L. Hudson, M.H. Moore, and Ariel Lewis, *Icarus*, 2010, **210**, 480.

[29] Y. Oba, N. Watanabe, A. Kouchi, T. Hama, and V. Pirronello, *ApJ*, 2010, **722**, 1598.

[30] Q. Zheng, and R. I. Kaiser, Chem. Phys. Lett., 2007, **450**, 55.

[31] C. E. Bryson and L. L. Levenson, *Surf. Sci*., 1974, **43**, 29.

[32] S. A. Sandford and L. J. Allamandola, *Icarus*, 1990, **87**, 188.

[33] P. U. Andersson, M. B. Nagard, G. Witt and J. B. C. Pettersson, *J. Phys. Chem*. *A*, 2004, **108**, 4627-4631.

[34] K. I. Öberg, E. C. Fayolle, H. M. Cuppen, E. F. van Dishoeck, and H. Linnartz, A&A, 2009, **505**, 183.

[35] J. T. Yardley, Laser chemistry: processing at the micro level. In: M. Bass and M.L. Stitch, Editors, Laser Handbook, Elsevier, Amsterdam, 1985, 405.

[36] J. F. Osmundsen, C.C. Abele and J.G. Eden, J. Appl. Phys., 1985, **57**, 2921.

[37] M. Seki, K. Kobayashi, and J. Nakahara, J. Phys. Soc. Jpn., 1981, **50**, 2643

[38] V. F. Petrenko, and R. W. Whitworth, Physics of Ice, Oxford Univ. Press, New York, 1999.

[39] O. Haida, T. Matsuo, H. Suga and S. Seki, J. Chem. Thermodynamics, 1974, **6**, 815.

[40] N. Watanabe, A. Nagaoka, T. Shiraki and A. Kouchi, *Astrophys. J*., 2004, **616**, 638.

[41] Y. Oba, N. Miyauchi, H. Hidaka, T. Chigai, N. Watanabe and A. Kouchi, *Astrophys. J*., 2009, **701**, 464.

[42] S. S. Prasad and S. P. Tarafdar, *Astrophys. J*., 1983, **267**, 603.

[43] M. H. Moore, R.L. Hudson and P.A. Gerakines, *Spectrochim. Acta, Part A*, 2001, **57**, 843.